

가

* . †

Densification behavior of metal powder under warm isostaic pressing with metal mold

JungGoo Park and KiTae Kim

Key Words : Densification(), Finite Element Analysis(), Metal Mold(), Metal Powder(), Warm Isostatic Pressing(), Warm Die Pressing()

Abstract

The effect of the metal mold on densification behavior of stainless steel 316L powder was investigated under warm isostatic pressing with metal mold. We use lead as metal mold and obtain experimental data of metal mold property. To simulate densification of metal powder, the elastoplastic constitutive equation proposed by Shima and Oyane was implemented into a finite element program (ABAQUS) under warm die pressing and warm isostatic pressing with metal mold. Finite element results were compared with experimental data for densification and deformation of metal powder under warm isostatic pressing and warm die pressing.

1. Pressing) 가 .⁽⁶⁾

가

(PM: Powder Metallurgy)

, (1-2)

가

가

가

(4-5)

가

가

(RIP: Rubber Isostatic

가 . Y. dai ⁽⁷⁾ -

, Park ⁽⁸⁾

*

†

Email: korean@postech.edu
Tel: (054) 279-2164 Fax: (054) 279-5899

Shima-Oyane ⁽⁹⁾

200°C 300°C 가 200°C, 300°C 가 400 MPa

2. 가 8 μm (stainless steel 316L, Pamco Co., Japan) 2.5 (13) (Rockwell FR-3, Future-Tech Corp., Japan) (11) Jeon (10)

2.1 가 1200°C 4 D ≥ 0.985 3.1 3. (1) $\dot{\epsilon}_{ij}^p = \lambda \frac{\partial \Phi}{\partial \sigma_{ij}}$

(MTS servo-hydraulic tester) 가 Φ λ Shima Oyane (9)

2.2 가 200°C 300°C 가 10°C/min 10⁻³/s (vacuum furnace) (LVDT)⁽¹⁷⁾가 $\Phi(\sigma, \bar{\epsilon}_m^p, D) = \left(\frac{q}{\sigma_m}\right)^2 + 2.49^2(1-D)^{1.028} \left(\frac{p}{\sigma_m}\right)^2 - D^5 = 0$ (2) p, q, σ_m $\bar{\epsilon}_m^p$ 가 \dot{D}

(tantalum sheet) 200°C 300°C 10⁻³ mm/s (9) ABAQUS⁽¹²⁾ Shima-Oyane UMAT (3) $\dot{D} = -D \dot{\epsilon}_{kk}^p$

2.3 가 43 mm, 5 mm, 60 mm, 43 mm 0.44 200°C 300°C 400 MPa 가 가

2.4 가 26 mm 가 Fig. 1 10⁻³ mm/s 가

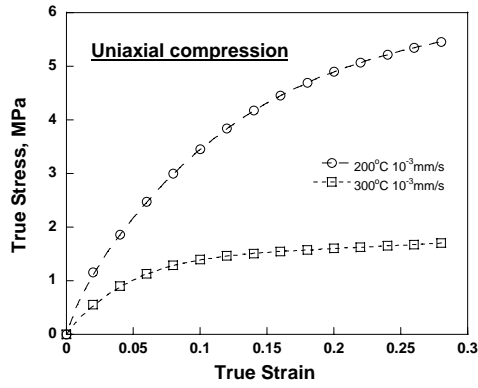


Fig. 1 Variation of true stress with true strain for lead specimen under uniaxial compression test at 200°C and 300°C

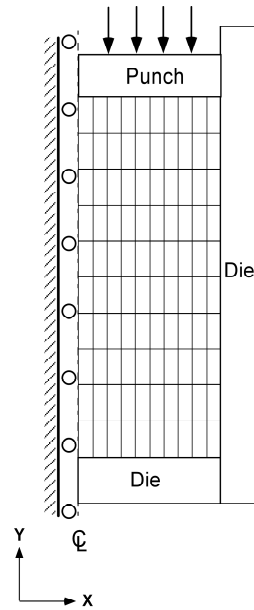


Fig. 2 Finite element meshes and boundary conditions for warm die pressing

offset
 E=14.35 GPa
 200°C
 E=35.20 GPa, 300°C
 0.45
 0.2%
 (16)

x
 1/2
 100 4 2
 CAX4(4-node axisymmetric quadrilateral, biquadratic displacement element)
 25
 RAX2(axisymmetric rigid element)
 (12)
 Shima-Oyane (9)

Fig. 3 0.17 가 (15-16)
 200°C 300°C

Ludwik
 200°C

$$\sigma_m = \begin{cases} 112.48 + 964.06(\bar{\epsilon}_m^p)^{0.57569} & (4) \\ 279.28 + 1377.3(\bar{\epsilon}_m^p)^{0.54997} & (5) \end{cases}$$

 300°C

$$\sigma_m = \begin{cases} 60.652 + 805.19(\bar{\epsilon}_m^p)^{0.4285} & (6) \\ 285.98 + 1214.4(\bar{\epsilon}_m^p)^{0.61821} & (7) \end{cases}$$

(9)
 (4) (6)
 (7)
 (5)

(5) (7) Shima-Oyane 가

4.4
Fig. 4

(16)
 0.33
 4.3
Fig. 2

x
 1/2
 100 124 4 2
 CAX4
 RAX2
 25 (12)

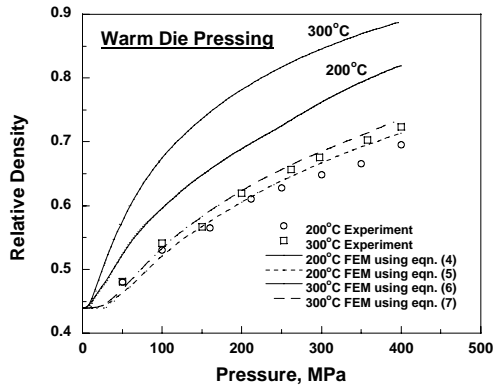


Fig. 3 Comparisons between experimental data and finite element results for the variation of relative density with axial stress during warm die pressing at 200°C and 300°C

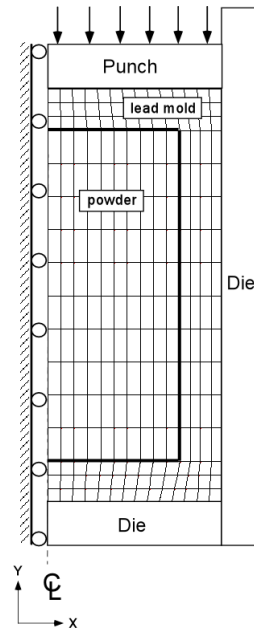


Fig. 4 Finite element meshes and boundary conditions for a powder compact in the metal mold isostatic pressing

Shima-Oyane
(9)

0.17 가
(14-15)
Fig. 5 200°C 300°C 가
가 300°C 가 (8)
60 mm, 43 mm 5 mm
0.44

200 °C 가 (14)
Fig. 6 300°C 250 MPa

4.5
4.5.1

(10)

$$D = 0.5559 + 0.00174 \cdot HRF + 1.089 \times 10^{-5} \cdot HRF^2 \quad (8)$$

4.5.2

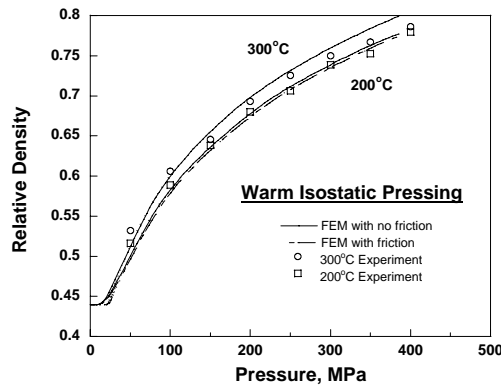


Fig. 5 Comparisons between experimental data and finite element results for the variation of relative density with axial stress during metal mold warm isostaitc pressing at 200°C and 300°C

Fig. 7 (a) (b) 200°C 250 MPa

Fig. 8 (a) (b) 300°C

200°C

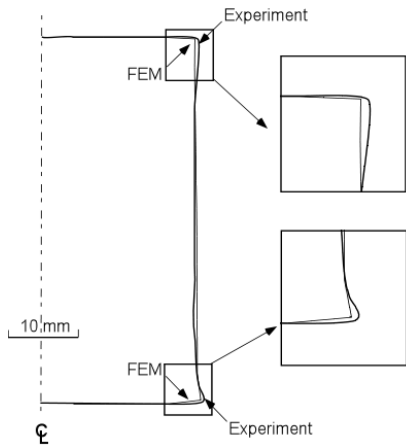


Fig. 6 Comparisons between experimental data and finite element result of deformation under 250 MPa during metal mold isostatic pressing at 300°C

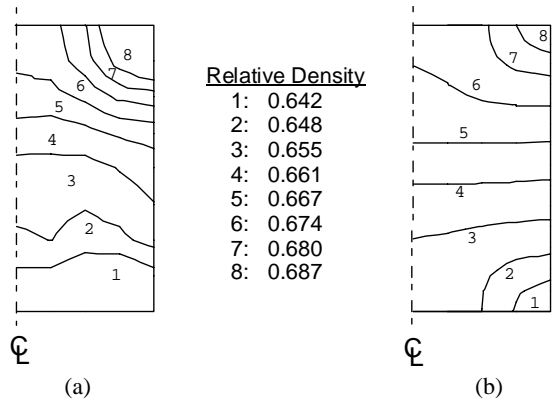


Fig. 8 Comparisons between (a) experimental data and (b) finite element result for relative density distribution under 250 MPa during warm die pressing at 300°C

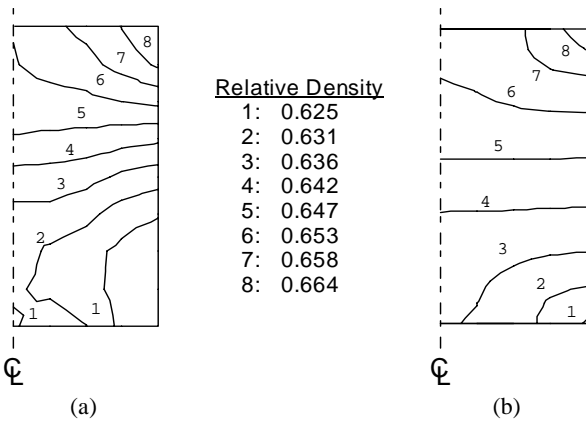


Fig. 7 Comparisons between (a) experimental data and (b) finite element result for relative density distribution under 250 MPa during warm die pressing at 200°C

4.5.3

Fig. 9 (a) (b) 200°C
250 MPa 가

Fig. 9(a)

Fig. 7

200°C

Fig. 10 (a) (b) 300°C
250 MPa 가

200°C

(1) Shima-Oyane

(9)

(2)

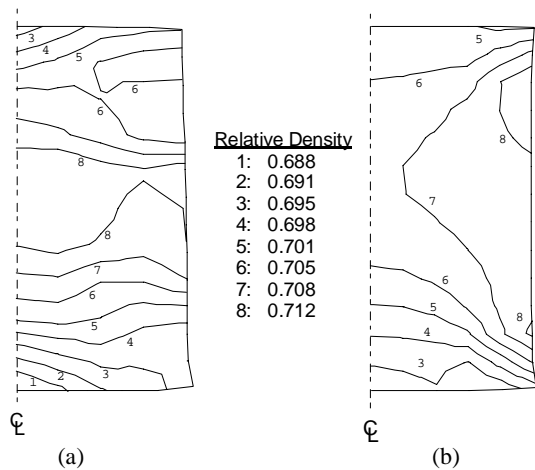


Fig. 9 Comparisons between (a) experimental data and (b) finite element result for relative density distribution under 250 MPa during metal mold isostatic pressing at 200°C

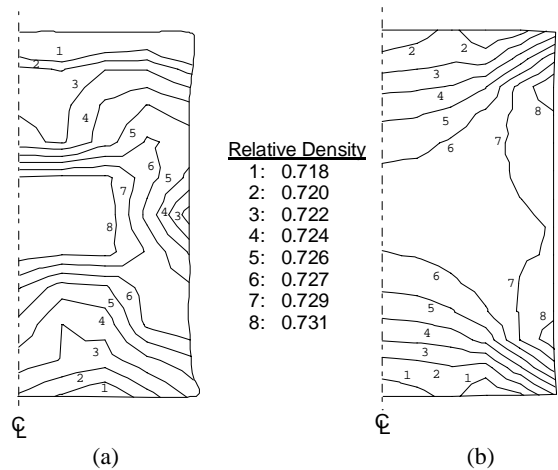


Fig. 10 Comparisons between (a) experimental data and (b) finite element result for relative density distribution under 250 MPa during metal mold isostatic pressing at 300°C

- (1) P. Arbstedt, 1986, "Developments in Iron and Steel Powder Production," *Metal Powder Reports*, Vol. 41, No. 1, pp. 64~67.
- (2) D. Whittaker, 1995, "PM Routes to High Performance Parts," *Metal Powder Reports*, Vol. 50, No. 1, pp. 14~24.
- (3) James, P. J., 1983, *Isostatic Pressing* Applied Sci. Publishers.
- (4) S. St Laurent and F. Chagnon, 1999, "Behaviour of steel powder mixtures processed by warm compaction," *Metal Powder Report*, Volume 54, Issue 3, pp. 42.
- (5) Jens Wahnschaffe, 1998, "New compaction approaches to higher density PM: warm or cold," *Powder Metallurgy*, Vol. 41, No. 4, pp. 250~252.
- (6) Yang, H. C., Kim, J. K. and Kim, K. T., 2003, "Effect of a rubber mould on densification and deformation of metal powder during warm isostatic pressing," *Powder Tech.*, accepted.
- (7) Y. Dai, F. Barbagallo and F. Groeschel, 2003, "Compression properties of lead-bismuth," *Journal of Nuclear Materials*, Vol. 317, Issues 2-3, pp. 252~255.
- (8) Park, C. Y., Yang, D. Y., Lee, K. H. and Eun, I. S., 1994, "Process Development of the Large size Dome Shape Forging-Products Using the Incremental and Combined Forming Method," *Transactions of KSME*, A18, No. 7, pp. 1685~1696.
- (9) Shima, S. and Oyane, M., 1976, "Plasticity Theory for Porous Metals," *Int. J. Mech. Sci.*, Vol. 18, pp. 285~291.
- (10) Jeon, Y. C. and Kim, K. T., 1999, "Near-net-shape forming of 316L stainless steel powder under hot isostatic pressing," *Int. J. Mech. Sci.*, Vol. 41, pp. 815~830.
- (11) Abe, O., Kanzaki, S., Ohashi, M. and Tabata, H., 1987, "Influence of size and shape on homogeneity of powder compacts formed by cold isostatic pressing (part 1): Press forming of thick cylinders," *International Journal of High Technology Ceramics*, Vol. 3, Issue 3, pp. 257~258.
- (12) ABAQUS User's I, II and III Manual, 2001, Ver. 6.2, H.D. Hibbitt, I. Karlsson and E.P. Sorenson, USA.
- (13) Yang, H. C., and Kim, K. T., 2000, "Densification Behavior of Ti-6Al-4V Powder Compacts by Hot Isostatic Pressing," *Transactions of KSME*, A24, No. 2, pp. 394~402.
- (14) Han, H. N., Lee, Y. G., Oh, K. H. and Lee, D. N., 1996, "Analysis of Hot forging of Porous Metals," *Mat. Sci. Eng. A*, A206, pp. 81~89.
- (15) Altan, T., Oh, S. I. and Gegel, H. L., 1983, *Metal Forming: Fundamentals and Application*, American Society for Metals, Metals Park, Ohio, pp. 1~353.
- (16) ASM Handbook Properties and selection: Nonferrous Alloys and Special-Purpose Materials, 1998, Vol. 2, Tenth edition.
- (17) Kim, J. H., Han, D. B. and Kim, K. T., 1996, "High temperature Creep Behavior of Cr₃C₂ Ceramic Composite," *Mat. Sci. Eng. A*, A212, pp. 87~93.